Liquid Crystals
Publication details, including instructions for authors and subscription information:
http://www.informaworld.com/smpp/title~content=t713926090

N,N-Disubstituted aminophenylazo-4-benzoates: preparation, mesogenic study, structure determination and molecular modelling

Long-Li Lai; Long-Je Lee; Gene-Hsiang Lee; Yu Wang; Kuang-Lieh Lu; Shwu-Jian Lee

To cite this Article Lai, Long-Li , Lee, Long-Je , Lee, Gene-Hsiang , Wang, Yu , Lu, Kuang-Lieh and Lee, Shwu-Jian(2001) '*N,N*-Disubstituted aminophenylazo-4-benzoates: preparation, mesogenic study, structure determination and molecular modelling', Liquid Crystals, 28: 10, 1513 — 1518

To link to this Article: DOI: 10.1080/02678290110071529

URL: http://dx.doi.org/10.1080/02678290110071529

Liquid Crystals, 2001, Vol. 28, No. 10, 1513–1518

N,*N*-Disubstituted aminophenylazo-4-benzoates: preparation, mesogenic study, structure determination and molecular modelling

LONG-LI LAI*, LONG-JE LEE
Department of Applied Chemistry, National Chi Nan University, Puli,
Taiwan 545, ROC

GENE-HSIANG LEE, YU WANG
Instrumentation Center and Department of Chemistry, National Taiwan
University, Taipei, Taiwan 106, ROC

KUANG-LIEH LU and SHWU-JIAN LEE
Institute of Chemistry, Academia Sinica, Taipei, Taiwan 115, ROC

(*Received 30 December 2000; in final form 8 May 2001; accepted 10 May 2001*)

A series of alkyl *N*,*N*-disubstituted aminophenylazo-4-benzoates were prepared from the reactions of an acyl phenylpiperazine with a series of the diazonium salts. The mesogenic behaviours of the resulting dyes were studied by polarizing optical microscopy and differential scanning calorimetry. Single crystal structure determination, powder XRD, and molecular modelling of a representative compound were also undertaken to understand the relative structural conformation.

1. Introduction

Azo dye molecules are attracting much attention in both academic and applications areas [1, 2]. In particular, azo-dyes have a reasonable dichroic ratio and are suitable for low power consumption reflective liquid crystal (LC) devices; the three-layered guest–host (G-H) systems are expected to be used for developing full colour reflective displays [3]. In these systems, the yellow, magenta, and cyan dyes are, respectively, incorporated into different liquid crystal cells. However, the dye solubility and the phase transition temperatures of the G-H systems are serious issues in applications studies. The clearing temperatures usually vary with the components of the G-H systems, and addition of the non-mesogenic dyes often causes instability of the corresponding LC phases [4]. Dyes which are themselves mesogenic minimize this effect; therefore azo dye liquid crystals are therefore highly desirable as dopants.

In previous work [5], we reported mesogenic studies on the azo dye derivatives **1** and **2** as shown in figure 1. We found that all the molecules showed smectic C phases, and that the mesogenic range seemed unrelated to the alkoxy chain length of the benzoate in the hydrogen bonded system **1**, or to the chain length of the carboxylate in compound **2**. This differs from our former observations in the quinoline system [6], in which the length of the alkoxy chain does affect the range of the smectic C phase. For a better understanding of these molecules, we have further synthesized compounds **5a**–**5e** (schemes 1 and 2), as these SmC phase-exhibiting materials have potential for ferroelectric or antiferroelectric devices. Compound **5b**, representatives of this series of molecules, was studied by single crystal structure determination, powder X-ray diffraction (XRD) and molecular modelling.

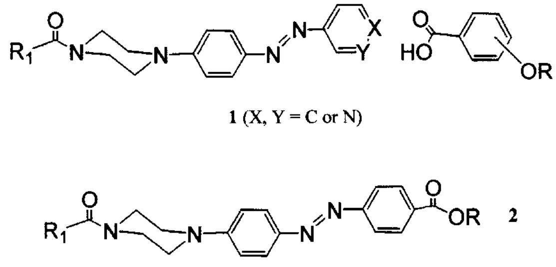

1 (X, Y = C or N)

2

Figure 1.

2. Experimental

The chemicals used in this work were commercially available from ACROS. High resolution mass spectra were obtained by a VG70-250S spectrometer (EI, 70 ev),

---

*Author for correspondence; e-mail: lilai@ncnu.edu.tw

Liquid Crystals ISSN 0267-8292 print/ISSN 1366-5855 online © 2001 Taylor & Francis Ltd
http://www.tandf.co.uk/journals
DOI: 10.1080/02678290110071529

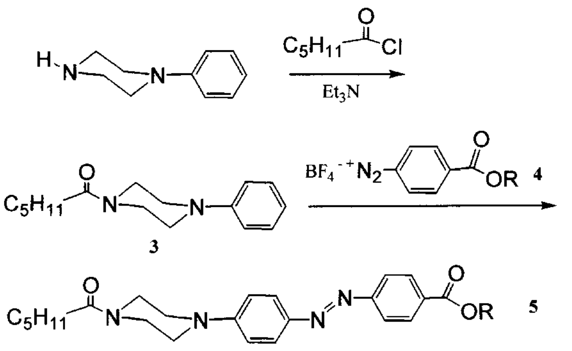

Scheme 1.

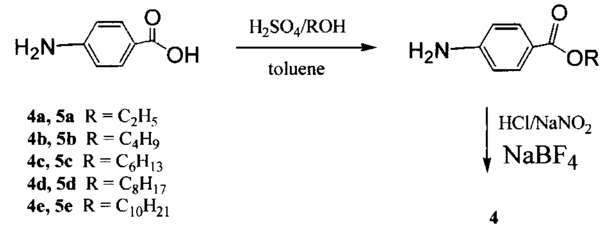

Scheme 2.

and ^1H NMR spectra were recorded on a Varian 200 FT NMR spectrometer. The mesogenic behaviours and phase transitions were characterized by polarizing optical microscopy (POM) and differential scanning calorimetry (Perkin-Elmer DSC 6). XRD patterns were obtained from a Siemens D-5000 X-ray diffractometer equipped with a TTK 450 temperature controller and a Cu radiation with the wavelength $\lambda = 1.5406$ Å. Semi-empirical calculation was carried out by the CAChe program, provided by Fujitsu (Japan). The structure of the molecule **5b** was optimized by performing a geometry calculation in mechanics using augmented MM3 parameters, and further refined by calculating the optimized geometry by MOPAC using PM3 parameters.

2.1. *Synthesis of the alkyl N,N-disubstituted aminophenylazo-4-benzoates 5*

N-Phenylpiperazine (8.05 g, 50 mmol) was dissolved in dry dichloromethane (100 ml). Dry triethylamine (10 ml), followed by hexanoyl chloride (6.73 g, 50 mmol) was then added at 0–5°C. The resulting solution was further stirred at room temperature for 30 min. NaOH (3 g) in water (50 ml) was added, and the solution was extracted with dichloromethane (50 ml). The combined extracts were dried over sodium sulphate and the solvent was removed under reduced pressure. Hexane (20 ml) was added to give *N*-hexanoyl-*N*′-phenylpiperazine **3** in an almost quantitative yield.

The phenylpiperazine derivative **3** (1.3 g, 2 mmol) and the corresponding diazonium salts **4** [7] (2.5 mmol) were added to a solution of acetic acid/water (15 ml, 2:1), and the solution was stirred at room temperature for 24 h. Water (100 ml) was added and the precipitated solid, was filtered off, washed with acetone (5 ml) and dried. The azo dyes **5**, after purification by chromatography for further physical study, were obtained in 50–70% yields. Products **5a**–**5d** were identified as the required materials and judged to be pure by ^1H NMR and high resolution mass spectroscopy. The following abbreviations and NMR spectra data are as follows: s = singlet, d = doublet, t = triplet, b = broad, J = coupling constant.

5a. ^1H NMR: δ ($CDCl_3$) 0.89 (t, 3H, CH_3), 1.29–1.78 (m, 9H, $3CH_2 + CH_3$), 2.36 (t, 2H, CH_2), 3.38 (s, b, 4H, $2CH_2$), 3.65 (t, 2H, CH_2), 3.79 (t, 2H, CH_2), 4.38 (quart, 2H, OCH_2), 6.96 (d, 2H, $J = 9.3$ Hz, 2 × Ar–H), 7.87 (d, 2H, $J = 8.4$ Hz, 2 × Ar–H), 7.91 (d, 2H, $J = 9.3$ Hz, 2 × Ar–H), 8.14 (d, 2H, $J = 8.4$ Hz, 2 × Ar–H). HRMS for $C_{25}H_{32}N_4O_3$ 436.2474; found 436.2476.

5b. ^1H NMR: δ ($CDCl_3$) 0.89 (t, 3H, CH_3), 1.03 (t, 3H, CH_3), 1.41–1.84 (m, 10H, $5CH_2$), 2.36 (t, 2H, CH_2), 3.38 (s, b, 4H, $2CH_2$), 3.65 (t, 2H, CH_2), 3.80 (t, 2H, CH_2), 4.33 (t, 2H, OCH_2), 6.96 (d, 2H, $J = 9.3$ Hz, 2 × Ar–H), 7.86 (d, 2H, $J = 8.4$ Hz, 2 × Ar–H), 7.91 (d, 2H, $J = 9.3$ Hz, 2 × Ar–H), 8.14 (d, 2H, $J = 8.4$ Hz, 2 × Ar–H). HRMS for $C_{27}H_{36}N_4O_3$ 464.2787; found 464.2787.

5c. ^1H NMR: δ ($CDCl_3$) 0.86–0.94 (m, 6H, $2CH_3$), 1.30–1.92 (m, 14H, $7CH_2$), 2.36 (t, 2H, CH_2), 3.38 (s, b, 4H, $2CH_2$), 3.66 (t, 2H, CH_2), 3.80 (t, 2H, CH_2), 4.32 (t, 2H, OCH_2), 6.96 (d, 2H, $J = 9.3$ Hz, 2 × Ar–H), 7.87 (d, 2H, $J = 8.4$ Hz, 2 × Ar–H), 7.91 (d, 2H, $J = 9.3$ Hz, 2 × Ar–H), 8.14 (d, 2H, $J = 8.4$ Hz, 2 × Ar–H). HRMS for $C_{29}H_{40}N_4O_3$ 492.3100; found 492.3102.

5d. ^1H NMR: δ ($CDCl_3$) 0.85–0.92 (m, 6H, $2CH_3$), 1.23–1.82 (m, 18H, $9CH_2$), 2.36 (t, 2H, CH_2), 3.38 (t, 4H, $2CH_2$), 3.65 (t, 2H, CH_2), 3.79 (t, 2H, CH_2), 4.32 (t, 2H, OCH_2), 6.96 (d, 2H, $J = 9.3$ Hz, 2 × Ar–H), 7.86 (d, 2H, $J = 8.4$ Hz, 2 × Ar–H), 7.91 (d, 2H, $J = 9.3$ Hz, 2 × Ar–H), 8.14 (d, 2H, $J = 8.4$ Hz, 2 × Ar–H). HRMS for $C_{31}H_{44}N_4O_3$ 520.3413; found 520.3411.

5e. ^1H NMR: δ ($CDCl_3$) 0.83–0.92 (m, 6H, $2CH_3$), 1.22–1.82 (m, 22H, $11CH_2$), 2.36 (t, 2H, CH_2), 3.38 (s, b, 4H, $2CH_2$), 3.65 (t, 2H, CH_2), 3.80 (t, 2H, CH_2), 4.32 (t, 2H, OCH_2), 6.96 (d, 2H, $J = 9.3$ Hz, 2 × Ar–H), 7.87 (d, 2H, $J = 8.4$ Hz, 2 × Ar–H), 7.91 (d, 2H, $J = 9.3$ Hz, 2 × Ar–H), 8.14 (d, 2H, $J = 8.4$ Hz, 2 × Ar–H). HRMS for $C_{33}H_{48}N_4O_3$ 548.3726; found 548.3727.

2.2. *X-ray crystallographic analysis*

Crystals of compound **5b** were grown from dichloromethane/hexane (1 : 1) at room temperature. A single crystal of suitable quality was mounted on a glass fibre and used for the measurement of precise cell constants and intensity data collection. Diffraction measurements were made on a Siemens SMART 1K CCD diffractometer with graphite-monochromated Mo-K$_\alpha$ radiation ($\lambda = 0.71073$ Å), operated at room temperature over the θ range 0.70–26.36°. No significant decay was observed during the data collection. A total of 6652 reflections were collected, yielding 4880 unique reflections; 3442 reflections were observed with $I \geqslant 2\sigma(I)$ reflections. Data were processed on a PC using the SHELXTL software package [8]. Systematic absences in the diffraction data of **5b** established the space group as $P2_1$. The structure of **5b** was solved using direct methods and refined by full-matrix least square on F^2 value. All non-hydrogen atoms were refined anisotropically. The hydrogen atoms were fixed at calculated positions and refined using a riding model. The final indices were $R1 = 0.0657$, $wR2 = 0.1347$ with goodness-of-fit = 1.075. The crystal data are summarized in table 1; selected bond lengths and angles are given in table 2.

3. Results and discussion

3.1. *Synthesis and mesogenic study*

The desired azo dye molecules **5a**–**5e** were synthesized as demonstrated in scheme 1. Compound **3** was obtained by reaction of *N*-phenylpiperazine with hexanoyl chloride in an almost quantitative yield. The diazonium salts **4a**–**4e** were prepared according to literature methods as described in scheme 2 [7]. The esterification process [9] gave about 60% yields, and the diazotisation was carried out in an almost quantitative yield. The mesogenic behaviours and phase transitions, characterized by POM and DSC are summarized in table 3. The smectic C phase appears during heating or cooling of the azo dye molecules; the mesogenic ranges are similar for either process (about 60–80°). The tilted SmC phase was characterized by the broken focal-conic fan texture coexisting with the schlieren texture. It was also confirmed by the XRD study. For example, *d*-spacings (the *Z* component of an extended molecular length) for compound **5b** are 28.16, 26.95, 26.73 and 26.69 Å at 200, 180, 160 and 150°C, respectively. In the SmC range, the tilt angle between the molecular and the *Z* axis decreases with increasing temperature, and the *d*-spacing thus becomes greater at the higher temperature.

Table 1. Crystallographic data for compound **5b**.

Formula	$C_{27}H_{36}N_4O_3$
Formula weight	464.60
Space group	$P2_1$
a/Å	5.8933(2)
b/Å	7.6031(3)
c/Å	29.1309(9)
β	92.826(1)°
v/Å^3	1303.69(8)
Z	2
D_c/g cm^{-3}	1.184
μ/cm^{-1}	0.78
$2\theta_{max}$/deg	52.72
Reflns measd	6652
Reflns used (R_{int})	4880(0.0286)
Final R [$I > 2\sigma(I)$]	$R1^a = 0.0657$, $wR2^b = 0.1347$
R (all data)	$r1 = 0.0930$, $wr2 = 0.1601$
Goodness-of-fit on F^2	1.075

[a] $R1 = \Sigma\,|F_0| - |F_c|/\Sigma\,|F_0|$

[b] $wR2 = [\Sigma w[(F_0^2 - F_c^2)^2]/\Sigma w(F_0^2)^2]^{1/2}$: $w = 1/[\sigma^2(F_0^2) + (0.08P)^2]$, where $P = [\max(F_0^2, 0) + 2F_c^2]/3$.

Table 2. Selected bond lengths (Å) and angles (°) for compound **5b**.

Bond lengths			
C1–C2	1.395(4)	C1–C6	1.401(4)
C1–N1	1.434(4)	C2–C3	1.383(4)
C3–C4	1.402(4)	C4–C5	1.400(4)
C4–C17	1.499(4)	C5–C6	1.383(4)
C7–C8	1.393(4)	C7–C12	1.400(4)
C7–N2	1.416(4)	C8–C9	1.386(4)
C9–C10	1.406(4)	C10–C11	1.416(4)
N1–N2	1.258(3)	O2–C18	1.469(3)
N2–C7	1.416(4)	O3–C22	1.233(4)
N3–C10	1.415(4)	N3–C13	1.467(4)
N3–C15	1.471(4)	N4–C22	1.360(4)
N4–C16	1.462(4)	N4–C14	1.465(4)
O1–C17	1.206(4)	O2–C17	1.346(4)
Bond angles			
C2–C1–N1	115.4(3)	C6–C1–N1	125.1(3)
C8–C7–N2	117.7(3)	C12–C7–N2	124.4(3)
O3–C22–N4	120.6(3)	O3–C22–C23	121.5(3)
N4–C22–C23	117.9(3)	N2–N1–C1	115.0(2)
N1–N2–C7	114.4(2)	C22–N4–C16	126.6(3)
C22–N4–C14	121.5(2)	C16–N4–C14	111.7(2)
C17–O2–C18	116.0(2)		

In previous work, we showed that nitrogen-containing heterocycles favour the formation of the SmC phase in LCS. Also, the chain length of the flexible part, which is related to the molecular stacking shape rather than the dipole moment, is important in enhancing the heterocyclic influence (to form an SmC phase with wider temperature range) [6]. However our present work shows that the chain length of the flexible carboxylate may not have a significant influence on widening the SmC phase. The C(=O)–N< moiety, introducing a strong dipole into the molecule, may be dominant in this case. Thus the chain length of the carboxylate moiety may have little effect on the molecular stacking.

3.2. *Structural determination and molecular modelling*

The structure of compound **5b** is shown in figure 2. The angles between plane C1–N2–N2–C7 and the two benzene rings (C1–C6 and C7–C12) are 6.73° and 6.87°, respectively. The rigid part of the molecule is almost planar. However, owing to the strong delocalization

Table 3. Phase transition temperature (°C) and corresponding enthalpies (J g^{-1}), in parentheses, of azo dyes **5**. The phase transition temperatures and corresponding enthalpies of **5** were determined by the 2nd DSC scans using Perkin Elmer DSC-6 at heating and cooling rates of 10°C min^{-1} between 45 and 240°C. Cr = crystalline, SmX = unidentified smectic phase, SmX′ = unidentified smectic phase, SmC = smectic C phase, I = isotropic liquid.

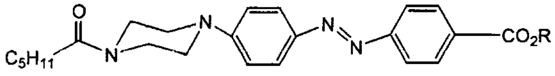

5

5a	$\mathrm{Cr} \xrightleftharpoons[65.7(3.4)]{115.7(15.0)} \mathrm{SmX} \xrightleftharpoons[131.0(0.7)]{149.4(0.3)} \mathrm{SmC} \xrightleftharpoons[213.0(7.1)]{217.7(7.9)} \mathrm{I}$
5b	$\mathrm{Cr} \xrightarrow{134.0} \mathrm{SmX'} \xrightleftharpoons[69.3(1.5)]{} \overset{136.7^{a}}{\underset{\mathrm{SmX}}{}} \xrightleftharpoons[135.0(0.5)]{} \mathrm{SmC} \xrightleftharpoons[201.3(7.3)]{207.4(10.5)} \mathrm{I}$
5c	$\mathrm{Cr} \xrightarrow{101.7(60.0)} \mathrm{SmX'} \xrightleftharpoons[75.7(3.4)]{117.4(1.4)} \mathrm{SmX} \xrightleftharpoons[132.3(1.8)]{134.1(2.4)} \mathrm{SmC} \xrightleftharpoons[201.6(20.8)]{203.4(22.9)} \mathrm{I}$
5d	$\mathrm{Cr} \xrightarrow{100.7(43.5)} \mathrm{SmX'} \xrightleftharpoons[78.6(11.4)]{109.0(5.2)} \mathrm{SmX} \xrightleftharpoons[134.6(1.3)]{132.7(1.6)} \mathrm{SmC} \xrightleftharpoons[198.0(16.7)]{200.4(18.9)} \mathrm{I}$
5c	$\begin{matrix}\mathrm{Cr}\\ \mathrm{SmX'}\end{matrix} \xrightleftharpoons[78.6(10.1)]{91.7(42.5)} \mathrm{SmX} \xrightleftharpoons[130.6(1.8)]{132.4(2.7)} \mathrm{SmC} \xrightleftharpoons[195.6(17.0)]{197.4(19.1)} \mathrm{I}$

[a] The peaks are overlapped and the total enthalpy is 18.3 J g^{-1}.

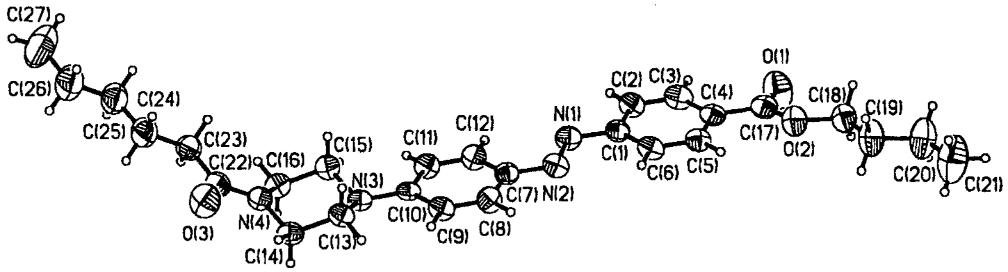

Figure 2. The molecular structure of compound **5b**, thermal ellipsoids drawn at the 50% probability level.

of the C(=O)–N< moiety itself, there is considerable bending between the piperazine and the acyl chain as shown in figure 3. On the basis of the crystallographic structure, the distance between C21 and C27 is 26.09 Å, which is quite close to the *d*-spacing from the XRD study 26.95 Å at 90°C (smectic X phase) and 170°C (smectic C phase).

The packing diagram for the intermolecular interaction of compound **5b** in the solid state is shown in figure 4. Compound **5b** is arranged in the head-to-tail position, i.e. the carboxylate end is directed toward the piperazine end; W-shaped packing is thus formed. The adjacent layers of the molecules are also arranged head-to-tail, but in the opposite direction, which may result from the influence of the piperazine unit. In such a packing, the congestion from two piperazine moieties can be avoided. From the literatures [10], we find that the *N*-substituents of the piperazine favour the equatorial conformation, and that the energy barrier between the equatorial and axial conformation is only 1.9–4 kcal mol^{-1}.

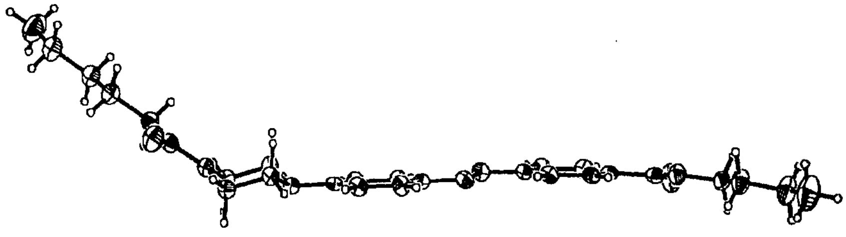

Figure 3. Horizontal view of compound **5b.**

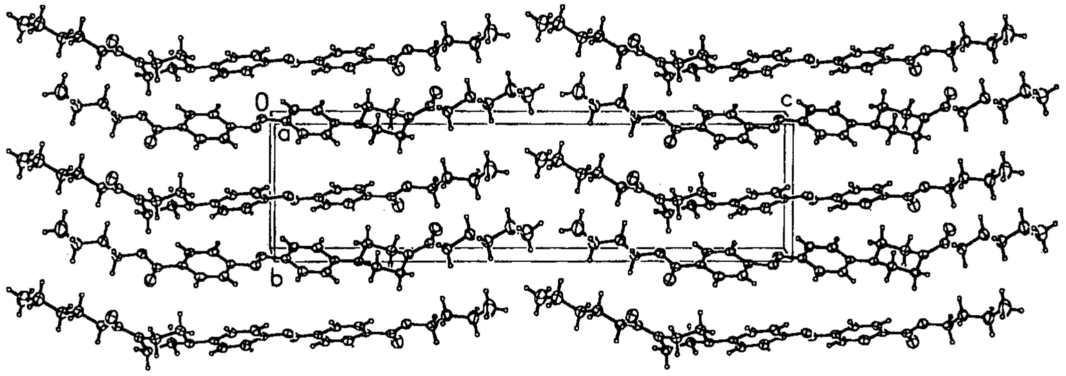

Figure 4. Packing diagram showing the intermolecular interaction of compound **5b** in the solid state.

Compound **5b** was also studied in more detail by semi-empirical calculation using the CAChe program. The structure of molecule **5b** was optimized by performing a geometry calculation in mechanics using augmented MM3 parameters and further refined by calculating the optimized geometry by MOPAC using PM3 parameters. After optimization, the length of molecule **5b** is 26.10 Å, in which the C=O moiety is directed in the equatorial position and the corresponding heat of formation is $-66.13\,\mathrm{kcal\,mol^{-1}}$ (figure 5). If the C=O functional group is directed in axial position as in figures 6 (*a*) or 6 (*b*), the molecular lengths are 25.62 and 26.38 Å, respectively, and the corresponding heats of formation are -66.10 and $-65.01\,\mathrm{kcal\,mol^{-1}}$. It seems there is no energy barrier between the figure 5 and figure 6 (*a*) structures, and the energy barrier between the figures 5 and 6 (*a*) conformation and the figure 6 (*b*) conformation is about $1.10\,\mathrm{kcal\,mol^{-1}}$, which is also small and consistent with literature values. We may therefore conclude that vibration of the >N–C=O group of compounds **5** in the mesogenic range likely happens, and that the conformation in figures 5 and 6 (*b*) may also exist, being more linear and favouring the formation of the LC phase.

We thank National Chi Nan University and National Science Council (NSC 89-2113-M-260-005) for financial support. The National Center of High-Performing Computing and Institute of Chemistry, Academia Sinica are also highly appreciated for providing the Beilstein data system and kind library service, respectively.

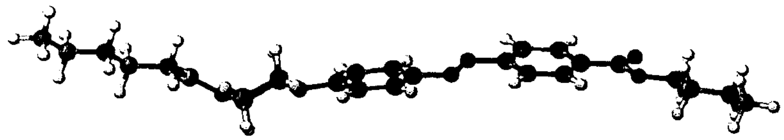

Figure 5. The optimized structure **5b** by CAChe program, in which the C=O group is at the equatorial position of the piperazine moiety. The corresponding heat of formation is -66.13 Kcal/mol and the distance of two ending carbons is 26.10 Å.

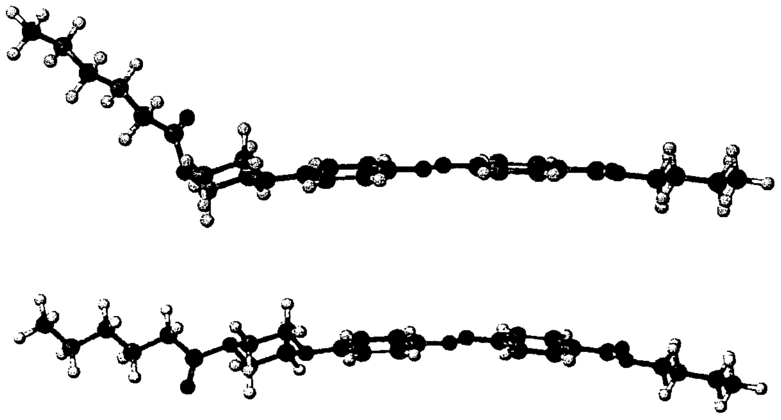

Figure 6. (*a*) The optimized structure **5b** by CAChe program, in which the C=O group is at the axial position of the piperazine moiety. The corresponding heat of formation is -66.10 Kcal/mol and the distance of two ending carbons is 25.62 Å. (*b*) The optimized structure **5b** by CAChe program, in which the C=O group is at the axial position of the piperazine moiety. The corresponding heat of formation is -65.01 Kcal/mol and the distance of two ending carbons is 26.38 Å.

References

[1] (*a*) Feringa, B. L., Van Delden, R. A., Koumura, N., and Geertsema, E. M., 2000, *Chem. Rev.*, **100,** 1789; (*b*) Kawata, S., and Kawata, Y., 2000, *Chem. Rev.*, **100,** 1777; (*c*) Delaire, J., and Nakatani, K., 2000, *Chem. Rev.*, **100,** 1817; (*d*) Ichimura, K., 2000, *Chem. Rev.*, **100,** 1847; (*e*) Tamai, N., and Miyasaka, H., 2000, *Chem. Rev.*, **100,** 1875; (*f*) Shirota, K., and Yamaguchi, I., 2000, *Liq. Cryst.*, **27,** 555.

[2] (*a*) Ruslim, C., and Ichimura, K., 1998, *Chem. Lett.*, 789; (*b*) Kozlovsky, M. V., Shibaev, V. P., Stakhanov, A. I., Weyrauch, T., and Haase, W., 1998, *Liq. Cryst.*, **24,** 759; (*c*) Shibaev, V. P., Kostomin, S. A., and Ivanov, S. A., 1996, in *Polymer as Electrooptical and Photooptical Active Media*, edited by V. P. Shibaev (Berlin: Springer), pp. 37–110; (*d*) Ikeda, T., and Tsutsumi, O., 1995, *Science*, **268,** 1873; (*e*) Anderle, K., and Wendorff, J., 1994, *Mol. Cryst. liq. Cryst.*, **243,** 51; (*f*) Hermann, D. S., Rudquist, P., Ichimura, K., Kudo, K., Komitov, L., and Lagerwall, S. T., 1997, *Phys. Rev. E*, **55,** 2857; (*g*) Sasaki, T., Ikeda, T., and Ichimura, K., 1994, *J. Am. chem. Soc.*, **116,** 625.

[3] (*a*) Sunohara, K., Naito, K., Tanaka, M., Naikai, Y., Kamiura, N., and Taira, K., 1996, *SID'96 Dig.*, 103; (*b*) Taira, K., Iwanaga, H., Hotta, A., Nakai, Y., Ohtake, T., and Sunohara, K., 1996, *AM-LCD'96*, 333; (*c*) Bauman, D., 1998, *Mol. Cryst. liq. Cryst.*, **159,** 197.

[4] (*a*) Naoum, M. M., Saad, G. R., Nessim, R. I., and Abdel Azis, T. A., 1998, *Liq. Cryst.*, **25,** 165; (*b*) Gray, G. W., 1962, *Molecular Structure and Properties of Liquid Crystals* (New York: Academic Press).

[5] (*a*) Lai, L. L., and Lin, H.-C., 2000, *Liq. Cryst.*, **27,** 707; (*b*) Lai, L. L., Wang, E., Lee, L. J., Chen, J. J., and Yang, D. W., 2001, *Liq. Cryst.*, **28,** 157; (*c*) Lai, L. L., Lee, L. J., Wang, E., and Su, F. Y., *Liq. Cryst.* (in the press).

[6] Lin, H.-C., Lai, L. L., Hsieh, W. P., and Huang, W. Y., 1997, *Liq. Cryst.*, **22,** 661.

[7] Schilling, M. L., Katz, H. E., and Cox, D. I., 1998, *J. org. Chem.*, **53,** 5538.

[8] Sheldrick, G. M., 1994, SHELXTL version 5.03, Siemens Analytical X-ray Instruments Inc., Madison Wisconsin, USA.

[9] Murza, M. M., Golovanov, A. V., and Safarov, M. G., 1995, *Russ. J. org. Chem. (Engl)*, **31,** 1529.

[10] (*a*) Baker, V. J., Ferguson, I. J., Katritzky, A. R., and Patel, R., 1976, *Tetrahedron Lett.*, 4735; (*b*) Niemeyer, H. M., 1979, *J. mol. Struct.*, **57,** 241.